Electron beam irradiation-induced transport and recombination in p-type gallium oxide grown on (001) β-Ga$_2$O$_3$ substrate

Gabriel Marciaga ; Jian-Sian Li ; Chao-Ching Chiang ; Fan Ren ; Stephen J. Pearton ; Corinne Sartel; Zeyu Chi ; Yves Dumont ; Ekaterine Chikoidze ; Alfons Schulte ; Arie Ruzin ; Leonid Chernyak ✉

Check for updates

🗎 CHORUS

View Online

Export Citation

AIP Publishing

Electron beam irradiation-induced transport and recombination in p-type gallium oxide grown on (001) β-Ga$_2$O$_3$ substrate

View Online   Export Citation   CrossMark

Gabriel Marciaga,[1] (ID) Jian-Sian Li,[2] (ID) Chao-Ching Chiang,[2] (ID) Fan Ren,[2] (ID) Stephen J. Pearton,[3] (ID) Corinne Sartel,[4]
Zeyu Chi,[4] (ID) Yves Dumont,[4] (ID) Ekaterine Chikoidze,[4] (ID) Alfons Schulte,[1] (ID) Arie Ruzin,[5] (ID)
and Leonid Chernyak[1,a] (ID)

AFFILIATIONS

[1]Department of Physics, University of Central Florida, Orlando, Florida 32816, USA
[2]Department of Chemical Engineering, University of Florida, Gainesville, Florida 32611, USA
[3]Department of Materials Science and Engineering, University of Florida, Gainesville, Florida 32611, USA
[4]Groupe d'Etude de la Matière Condensée, Université Paris-Saclay, Université de Versailles Saint Quentin en Yvelines—CNRS,
45 Av. des Etats-Unis, Versailles Cedex 78035, France
[5]School of Electrical Engineering, Tel Aviv University, Tel Aviv 69978, Israel

[a]Author to whom correspondence should be addressed: leonid.chernyak@ucf.edu

ABSTRACT

This study investigates minority electron diffusion length and carrier recombination phenomena in p-type 300 nm-thick Ga$_2$O$_3$ films homo-epitaxially grown over a (001) tin-doped β-Ga$_2$O$_3$ conductive substrate. This research is novel due to its systematic and near-simultaneous measurements in the top layer of a p-Ga$_2$O$_3$/n-Ga$_2$O$_3$ structure using independent electron beam-induced current and cathodoluminescence techniques. Previous work primarily focused on heteroepitaxial architectures or gallium oxide grown over insulating substrates of the same material. In this work, the activation energies related to point defects in gallium oxide were extracted from temperature-dependent incremental electron beam irradiation experiments to gain insight into the defect landscape and its influence on minority carrier transport and recombination dynamics.

I. INTRODUCTION

Electron beam excitation significantly impacts the diffusion length and cathodoluminescence in gallium oxide (Ga$_2$O$_3$), a wide-bandgap semiconductor with promising applications in optoelectronics and power electronics. The effects are primarily attributed to generation (under the influence of electron beam) of non-equilibrium carriers in the material and their interaction with defects.[1]

Electron beam irradiation generally leads to a significant elongation of minority carrier diffusion length (L) in both n-type and p-type Ga$_2$O$_3$.[1,2] This increase follows a linear trend with the duration of electron beam irradiation before eventually saturating.[3]

The mechanism for the elongation of L under electron irradiation is attributed to the trapping of non-equilibrium carriers

(generated by the primary electron beam) by neutral gallium vacancies which create metastable deep acceptor levels within the bandgap of Ga$_2$O$_3$.[1] By occupying these defect levels, the non-equilibrium carriers (electrons in p-Ga$_2$O$_3$) effectively passivate the defects, preventing them from acting as recombination centers for carriers and, thus, leading to an increase in carrier lifetime (τ).[1]

With fewer recombination centers available, non-equilibrium minority carriers experience a longer τ and can travel a greater average distance before recombining with majority carriers. The diffusion length is related to the diffusion coefficient (D) and the carrier lifetime via the following equation:[4]

$$L = \sqrt{D\tau}. \tag{1}$$

18 August 2025 00:33:35

Therefore, an increase in carrier lifetime directly translates to a longer diffusion length.

Interestingly, electron beam irradiation has also been shown to recover the diffusion length in Ga_2O_3 samples that have been previously degraded by radiation (e.g., alpha and proton irradiation).[2] In some cases, the diffusion length after electron beam exposure even surpasses the values prior to high-energetic particles irradiation, indicating not only a "healing" effect of the electron beam, but also a fundamental improvement of the material.

The rate of increase in diffusion length with electron irradiation and L saturation behavior are temperature-dependent, suggesting that the trapping and de-trapping processes at the defect levels are thermally activated. Activation energies for these processes, linked to gallium vacancy-related defects,[3,5] have been estimated in the range from 72 to 304 meV using EBIC and CL techniques.

Studies have shown that the intensity of CL emission bands can decrease with increasing duration of electron beam irradiation.[5] This decay is linked to the trapping of non-equilibrium electrons at defect levels, which are also involved in radiative recombination processes. By trapping these electrons, the availability of these levels for radiative transitions is reduced, leading to a decrease in CL intensity.[6–17]

Prior investigations studied the electron irradiation-induced effects in undoped epitaxial p-type gallium oxide grown on (010)-oriented insulating Fe-doped Ga_2O_3 substrates.[3,5] In contrast, this work examines minority carrier diffusion length and recombination phenomena using two complementary techniques—electron beam-induced current and cathodoluminescence—in undoped p-type Ga_2O_3 thin films grown on conductive (001)-oriented gallium oxide substrates doped with tin (Sn). Previous and current work may, therefore, highlight similarities and differences in minority carrier transport and recombination dynamics in epitaxial p-type Ga_2O_3 of different crystallographic orientations.

II. EXPERIMENTAL

The undoped 300 nm-thick p-type β-Ga_2O_3 epilayer was grown on n-type ($\sim10^{19}$ cm^{-3} electron concentration) Sn-doped β-Ga_2O_3 (001) substrates (purchased from Novel Crystal Technology) by Metal-Organic Chemical Vapor Deposition (MOCVD). Trimethylgallium (TMGa) as a source for gallium and high-purity oxygen gas were used as precursors. The flow rates of TMGa and O_2 were set at 34 μmol/min and 3200 SCCM, respectively. The pressure and temperature in the growth chamber were maintained at 40 Torr and 825 °C. The ionized acceptor density in the epilayer between 40 and 200 nm from the top surface was estimated between 1.1×10^{17} and 3.0×10^{17} cm^{-3} by capacitance–voltage (C–V) measurements (cf. Fig. 1). A w-shape concentration profile, observed between 80 and 140 nm, may reflect a local variation in native acceptor creation during growth or a localized charge accumulation region.

While many types of Ga_2O_3-based p–n heterojunctions have been demonstrated, there is still interest in p–n homojunctions. It should be noted that epitaxial growth of p-type β-Ga_2O_3 on the n-type (001) gallium oxide substrate, reported in this work, represents one of the first attempts for homoepitaxial p–n junction realization. p-SiC/n-Ga_2O_3, p-GaN/n-Ga_2O_3, p-NiO$_x$/n-Ga_2O_3,
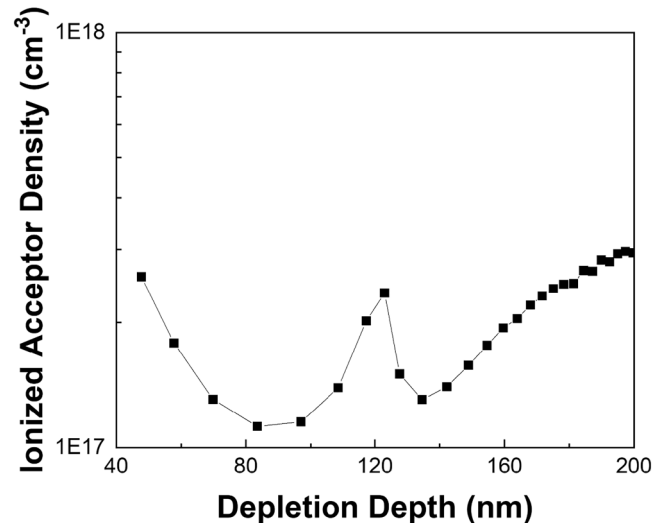

FIG. 1. Ionized acceptor density measured at 450 K in the top p-type epilayer obtained between 40 and 200 nm of depth from the surface using capacitance–voltage (C–V) measurements.

LiGa$_5$O$_8$, and p-diamond/n-Ga_2O_3 heterojunctions are reported in Refs. 18–28. Among these heterojunctions, the p-NiO/n-Ga_2O_3 heterojunction rectifiers have breakdown voltages up to 13.5 kV.[29] Realization of Ga_2O_3 p–n homojunctions should offer superior lattice and band alignment over heterojunctions, which minimizes interfacial defects and improves carrier transport efficiency.[30,31] This, in turn, should lead to higher breakdown voltages, as the absence of heterointerface discontinuities allows for a more uniform electric field distribution under reverse bias. Additionally, Ga_2O_3 homojunctions should demonstrate better thermal stability by avoiding the thermal expansion mismatch issues inherent in heterojunctions. Finally, homojunction fabrication is simpler and circumvents heteroepitaxial growth and dopant interdiffusion. The development of reliable p-type Ga_2O_3 remains a significant hurdle, and that is why p-NiO currently provides an available alternative.[26,28,29] Advances in nitrogen-doping could pave the way for more practical Ga_2O_3 homojunctions in the future.[30]

Huang et al.[31] reported that p-type Ga_2O_3 was created using phosphorus ion implantation into undoped epilayers, with subsequent rapid thermal annealing at 1100 °C. The n-type Ga_2O_3 epilayers were then regrown onto these layers. Diode structures showed clear evidence of rectification. Liu et al.[32] reported p–n homojunction structures in which the β-Ga_2O_3 films were produced by thermally oxidizing GaN films at 1150 °C in oxygen using a chemical vapor deposition system, resulting in p-type N-doped β-Ga_2O_3 through structural phase transitions. The doping type (p- or n-type) depended on the pre-doped impurities (N or Si) in the GaN substrates.

An additional characterization of p–n junction structures grown in this work is presented in Figs. S1–S3 in the supplementary material, which show a schematic of the diode structure (S1) used for C–V (S2) and I–V measurements (S3). Rectification signatures

are clearly observed in these figures. Pending detailed studies of Ga_2O_3 p–n homojunctions fabricated by this team, the research reported here is focused on studies of the top p-type epitaxial layers grown on the n-type (001) gallium oxide substrate using CL and EBIC techniques.

Cathodoluminescence characterizations were conducted across a 50–120 °C temperature range with the electron beam operated at an acceleration voltage of 20 kV utilizing a Gatan MonoCL2 attachment on the SEM. The temperature-dependent cathodoluminescence spectra were obtained using a temperature-controlled stage connected to an external control unit. Emitted light was detected with a Hamamatsu photomultiplier tube (sensitive over 150–850 nm) following dispersion by a single-grating monochromator (1200 lines/mm blaze).[6]

Electron beam-induced current measurements performed *in situ* in a Phillips XL-30 SEM were used to determine minority carrier diffusion length. This technique utilizes planar line-scan electron beam excitation, with the beam traversing the sample's surface.[1,2,7–9] EBIC characterizations were conducted across a 25–120 °C temperature range under an electron beam accelerating voltage of 25 kV, which ensures full penetration into the epitaxial p-type layer. The corresponding ~0.6 nA absorbed current was measured with a Keithley 480 pico-ammeter, and the electron range in the material was estimated up to 1 μm.[10] For the diffusion length measurements, 16.3 μm lateral EBIC line-scans were performed outward from the edge of asymmetrical pseudo-Schottky contacts. These contacts were made of Ni/Au (20/80 nm) on the top p-type layer using standard lithography and liftoff techniques. It should be noted that although the thickness of the p-Ga_2O_3 epitaxial film under investigation is about 300 nm and the electron beam penetration depth is about 1000 nm, the diffusion length measurements are still reliable. This is because both contacts used for the measurements are located on the top surface of the structure ensuring the current path is laterally constrained within the p-type epitaxial layer.

Each individual line-scan requires ~12 s to be completed, which is on the one hand, adequate for determining L, and on the other hand, is short enough to minimize the impact of electron beam irradiation on the diffusion length during the EBIC measurements. The attenuation of the EBIC signal is expressed with the following relationship:[11–13]

$$I(d) = I_0 d^\alpha \exp\left(-\frac{d}{L}\right). \tag{2}$$

In the equation above, $I(d)$ is the EBIC signal at a given position, d, and the variable d is the distance measured outward from the Ni/Au contact edge. I_0 denotes a scaling factor. α is a coefficient for recombination. It should be noted that the value of α depends on the surface recombination velocity, v_s. It varies from $\alpha = -1/2$, for $v_s = 0$, to $\alpha = -3/2$, for $v_s = \infty$. Since infinite surface recombination velocity is very unlikely, in view of excellent luminescence efficiency of the samples, $\alpha = -1/2$ was used in this work.[7]

III. RESULTS AND DISCUSSION

Figure 2 presents the initial, pre-irradiation dependence of the EBIC signal at ambient temperature illustrating the exponential
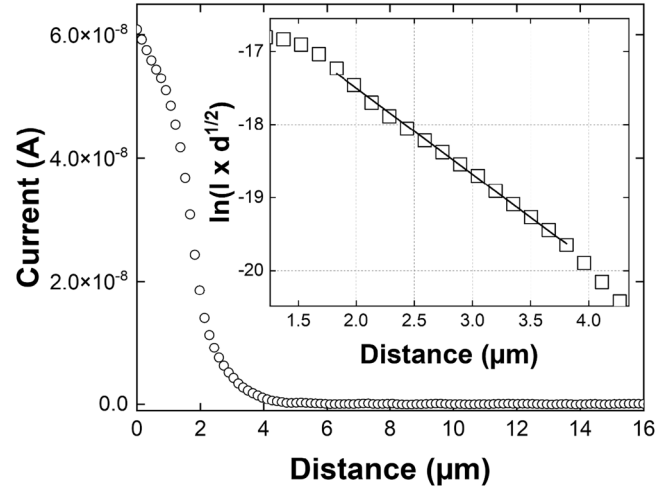
FIG. 2. Room temperature characteristics of the initial EBIC signal decrease as a function of distance from the Schottky contact's edge. The inset displays ln ($I \times d^{1/2}$) vs d, in accordance with Eq. (2). The minority carrier diffusion length, L, is calculated from the negative reciprocal of the linear fit's slope.

decay with increasing distance from the Schottky barrier edge. The inset plots $\ln(I \times d^{1/2})$ vs d for the derivation of L, according to Eq. (2). At room temperature, the negative reciprocal slope of the linear fit yields $L = 0.85 \mu$m. To investigate the impact of sustained carrier injection, the EBIC measurement line-scan region was exposed to continuous electron beam irradiation, accumulating to a total time of 1200 s. During the prolonged period of irradiation, diffusion length was periodically extracted using Eq. (2) at 100 s intervals up to the total 1200 s. It is important to note that at each temperature, the measurement was done at different pristine regions near the contact to avoid unintentional effects from previous tests.

Figure 3 illustrates the relationship between L and T, which reveals a decrease in L with increasing temperature. This was achieved via initial L measurements prior to continuous electron beam irradiation of the sample. This agrees with previous reports on Ga_2O_3,[2,12,13] where such behavior is ascribed to effects of phonon scattering. The thermal evolution of L is modeled by[9,12]

$$L(T) = L_0 \exp\left(\frac{\Delta E_{A,T}}{2kT}\right). \tag{3}$$

In this equation, L_0 is a scaling constant; $\Delta E_{A,T}$ is the associated thermal activation energy for this process; k is the Boltzmann constant; and T is the temperature. The value of $\Delta E_{A,T}$ can be extracted by linearizing Eq. (3) through a plot of $\ln(L)$ vs $1/(2kT)$ as seen in the inset of Fig. 3. This activation energy, characterizing the temperature-induced reduction in diffusion length, was determined to be 24 meV.

The results of the sustained electron beam irradiation EBIC experiments conducted at 25, 50, 75, 100, and 120 °C are presented in Fig. 4. The data acquired across this temperature range
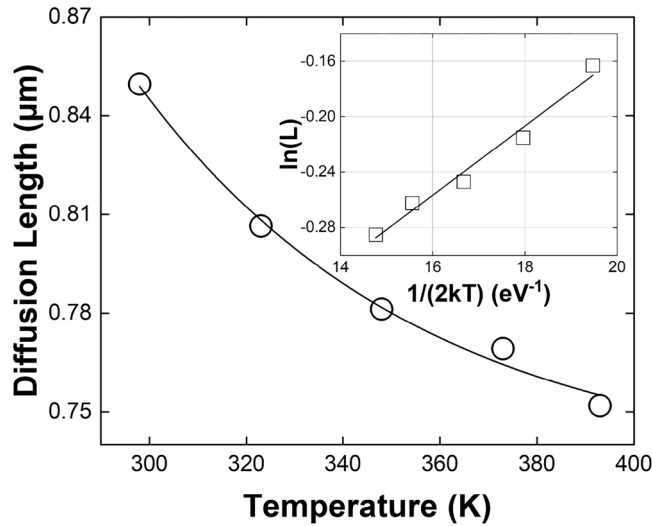
FIG. 3. Minority carrier diffusion length, L, vs temperature over a 25–120 °C range. The data demonstrate the expected exponential trend consistent with Eq. (3). The inset presents an Arrhenius plot of ln(L) vs 1/(2kT). $\Delta E_{A,T}$ of 24 meV was extracted using Eq. (3).

consistently show that L progressively increases with the cumulative total duration of electron beam irradiation (L saturation is not shown). A similar effect was previously observed in various wide-bandgap semiconductors such as p-Ga$_2$O$_3$, p-AlGaN, n-Ga$_2$O$_3$,
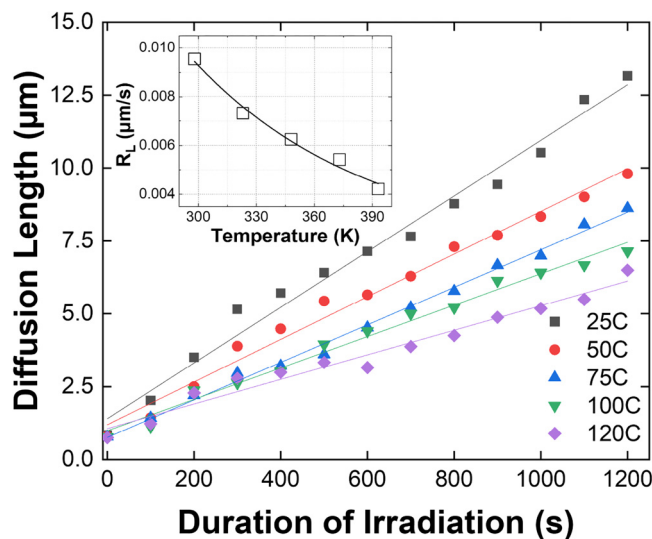

FIG. 4. Minority carrier diffusion length as a function of electron beam irradiation duration, measured at 25, 50, 75, 100, and 120 °C. The rate of diffusion length change, R_L, for each temperature is obtained as a slope from respective linear fits. The inset presents the relationship between R_L and temperature and the corresponding exponential fit according to Eq. (4).

p-ZnO, and unintentionally doped GaN.[2,8,9,16,17] The elongation of L seen in Fig. 4 is characterized by its rate of change, R_L, with respect to irradiation time. The inset of Fig. 4 highlights the relationship between R_L and temperature. The rate R_L drops from 9.5 nm/s at 25 °C to 4.5 nm/s at 120 °C. This temperature dependence of R_L is given by[2]

$$R_L = R_0 \exp\left(\frac{\Delta E_{A,T}}{2kT}\right)\exp\left(\frac{E_{A,I}}{kT}\right). \qquad (4)$$

For this equation, R_0 is a scaling constant, $\Delta E_{A,T}$ is the same as in Eq. (3), and $\Delta E_{A,I}$ is the activation energy associated with electron irradiation-induced process. Consequently, because Eq. (3) models the thermal dependence of L, it can be leveraged here to isolate and determine the activation energy of the irradiation-driven enhancement of L.

The Arrhenius plot presented in Fig. 5, where the slope corresponds to $\Delta E_{A,I} + 0.5\Delta E_{A,T}$, allows for the thermal and irradiation contributions to the elongation of L to be separated. Utilizing this relation, $\Delta E_{A,I}$ was determined to be 68 meV, which is associated with the mechanism for L elongation due to continuous electron irradiation. While this activation energy agrees well with that of Ref. 3 for undoped p-type Ga$_2$O$_3$ grown on the insulating (010)-oriented Fe-doped gallium oxide substrate ($\Delta E_{A,I} = 72$ meV), it is lower than in the previous report on highly resistive p-type Ga$_2$O$_3$ grown on sapphire ($\Delta E_{A,I} = 91$ meV).[2] The lower $\Delta E_{A,I}$, observed in this work for p-type Ga$_2$O$_3$ as compared to Ref. 2, may be indicative of a higher acceptor concentration present in the material. Acceptor levels create a band in the gallium oxide forbidden gap. Larger (as compared with highly resistive p-Ga$_2$O$_3$) majority carrier concentration in the material corresponds to a
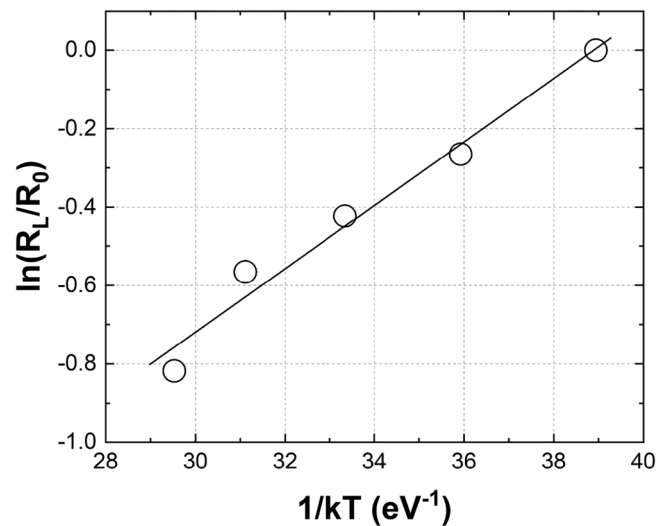
FIG. 5. The Arrhenius plot presenting ln(R$_L$/R$_0$) vs 1/kT. The linear fit's slope yields an activation energy of 68 meV via Eq (4).

18 August 2025 00:33:35

wide band for acceptors and, therefore, levels which are shallower may participate in the electron irradiation-induced effects.

An estimate for acceptor concentration (N_A; likely attributed to a gallium vacancy-related acceptor) is obtained in this work using the extracted from the EBIC analysis activation energy of 68 meV. The Hall measurements in Fig. 1 established a majority carrier (hole) density of about $2 \times 10^{17}\,\text{cm}^{-3}$ at 450 K. Utilizing this for the estimate, N_A was found to be $1.15 \times 10^{18}\,\text{cm}^{-3}$ calculated from the following equation:[4]

$$p(T) = N_A \exp\left(-\frac{\Delta E_{A,I}}{kT}\right). \tag{5}$$

Reference 1 presents a model for the sustained irradiation effects observed in this work. The energetic placement of certain deep defects within the Ga_2O_3 bandgap ensures they are predominately in a neutral charge state under equilibrium conditions. These deep defects can function as metastable traps for non-equilibrium carriers generated by an electron beam. Capturing a non-equilibrium carrier reduces the probability of further recombination via these deep states. Reduction in recombination leads to a longer carrier lifetime for the non-equilibrium charge population. The corresponding increase in L is consistent with Eq. (1). Increasing temperature leads to escape of captured carriers from deep traps, as the former overcome a local potential barrier associated with metastability. As a result, these deep traps become again available for recombination, but the rate R_L decreases with increasing temperature.

It should be noted that although EBIC technique does not provide direct proof for p-type electrical conductivity in the epitaxial layers under test, the absolute values for L (electrons) in these layers are —two to three times longer as compared to the diffusion length for holes measured in Refs. 9 and 13, thus providing an indirect proof for majority hole conductivity.

While EBIC reveals how far carriers can travel before recombination, it does not distinguish between radiative and non-radiative recombination processes. To complement the EBIC technique, temperature-dependent CL measurements were carried out to obtain more information about radiative efficiency and the thermal activation energies of competing non-radiative pathways in Ga_2O_3. These two methods allow for a more complete picture of the minority carrier dynamics and defect landscape in the epitaxial p-Ga_2O_3.

Figure 6 presents the evolution of CL spectra acquired continuously at 50 °C from a $10\,\mu m^2$ area on the p-type Ga_2O_3 epitaxial surface under electron beam irradiation. The observed CL spectra are characteristic of β-Ga_2O_3, predominantly consisting of several broad emission bands rather than distinct near-band edge emission. The broad emission bands in β-Ga_2O_3 are typically attributed to defect complexes involving oxygen and gallium vacancies, alongside oxygen and gallium interstitials. Several comprehensive studies of n- and p-type Ga_2O_3 optical properties have been presented in Refs. 12 and 14. Figure 6 shows a progressive decay in the overall CL intensity with increasing electron irradiation duration.

The peak CL intensity at 50 °C, extracted from spectra presented in Fig. 6, is plotted against electron beam irradiation
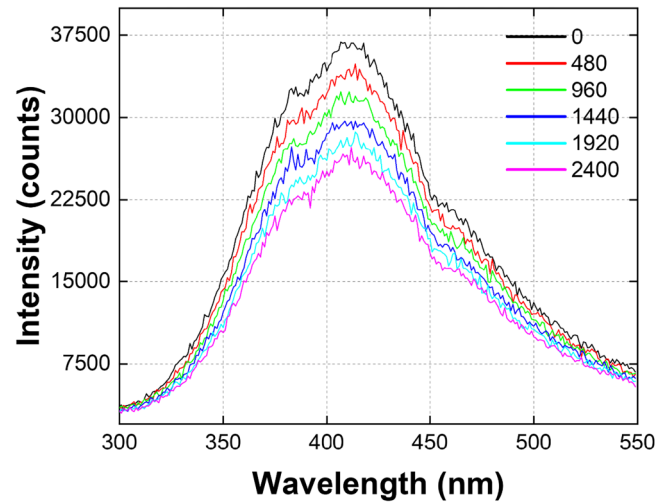
FIG. 6. Evolution of CL spectra from a p-Ga_2O_3 epitaxial layer at 50 °C under prolonged electron beam irradiation. The initial spectrum (black) corresponds to the initial near zero duration of irradiation. Subsequent spectra were taken in 480 s intervals up to 2400 s.

duration and is presented in the inset of Fig. 7. This agrees with the previous CL report on p-type Ga_2O_3 in which both CL and EBIC were measured in the same area to demonstrate (prior to saturation effects) the near-linear enhancement of L and corresponding CL

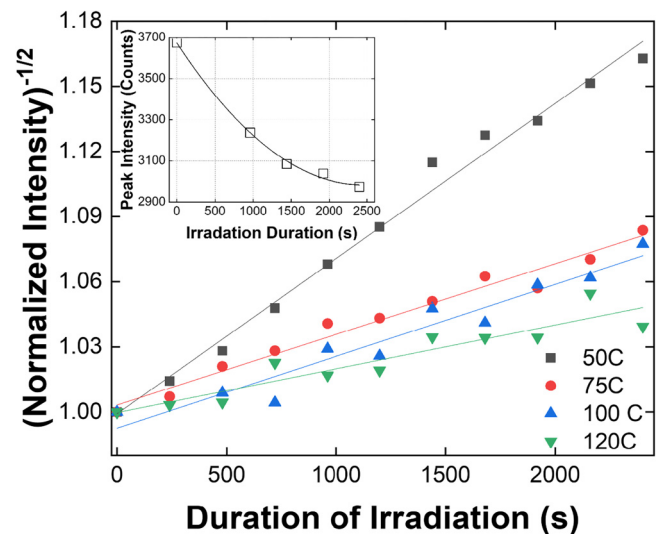**FIG. 7.** Electron beam irradiation effects on the normalized CL peak intensity [presented as (normalized intensity)$^{-1/2}$] across a 50–120 °C range. The CL decay rates, R_{CL}, are given by the slopes of the linear fits for each temperature. The inset illustrates the $1/t^2$ dependence of the unnormalized CL peak intensity as a function of irradiation duration for the 50 °C measurement.
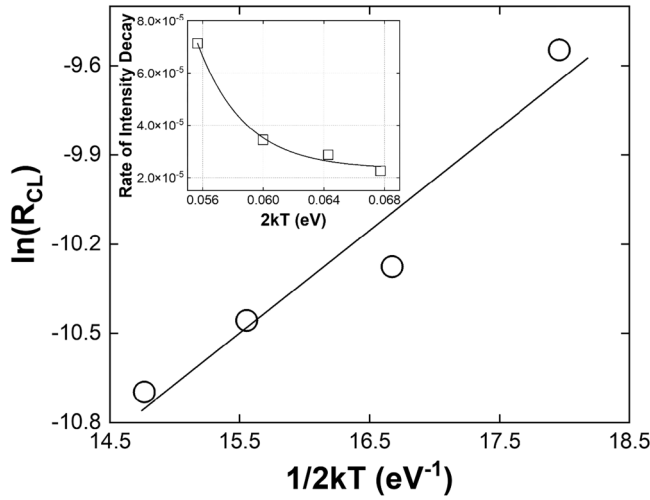
FIG. 8. Arrhenius plot presenting $\ln(R_{CL})$ vs $1/(2kT)$ dependence. The linear fit's slope yields the activation energy ΔE_A. The inset depicts the relationship between R_{CL} vs 2kT according to Eq. (6).

peak intensity decrease.[5] Other reports on highly resistive p-type and n-type Ga_2O_3, and the mechanism responsible for sustained irradiation-induced effects on carrier recombination are detailed in Refs. 2 and 14.

Because L increases linearly with increasing duration of electron irradiation, t, (cf. Fig. 4), a peak CL intensity, I, (note: not the EBIC signal), is expected to be proportional to $1/t^2$, in accordance with Refs. 6 and 15. This is illustrated in the inset of Fig. 7. Considering $\tau \sim I^{-1.15}$ and the linear dependence of $\tau^{1/2}$ on t [cf. Fig. 4 and Eq. (1)], one should expect a linear relationship between $I^{-1/2}$ and electron irradiation duration. This is validated and presented in Fig. 7 for temperatures ranging from 50 to 120 °C. Note that the span of CL decay, presented in Fig. 6, diminishes at higher temperatures. The rate R_{CL} of CL decay for each temperature is the slope for each linear dependence. R_{CL} vs T for the sample under investigation, shown in the inset of Fig. 8, was fitted using the following equation:[2]

$$R_{CL} = R_0 \exp\left(\frac{\Delta E_A}{2kT}\right). \qquad (6)$$

In Eq. (6), R_0 is the scaling constant; ΔE_A is the activation energy for CL intensity decay; k is the Boltzmann constant; and T is the temperature. The value of ΔE_A was obtained from the slope of the Arrhenius plot shown in Fig. 8 and determined to be 344 meV.

Existing literature[33–43] provides comprehensive summaries of trap states in Ga_2O_3, which are frequently linked to native crystalline imperfections and native defects like gallium and oxygen vacancies (V_{Ga} and V_O, respectively). In Ref. 37, V_{Ga}-related energetic levels are reported at 100–300 and 300–500 meV above the top of the valence band maximum. This is in line with the CL

activation energies found in this work and a prior investigation of homoepitaxial p-type Ga_2O_3 grown on an insulating (010) substrate, where an activation energy of 304 meV was found.[5] ΔE_A of 344 meV obtained in this work is directly comparable to Ref. 5 and gives the same indication of deep defect levels.

IV. CONCLUSIONS

This investigation employed Electron Beam-Induced Current (EBIC) to characterize the minority electron diffusion length in undoped, homoepitaxial p-type gallium oxide grown on a conductive (001) Sn-doped substrate. Measurements were carried out across a temperature range of 25–120 °C and under electron irradiation durations totaling up to 1200 s. This revealed two trends: a continuous decrease in L with increasing temperature and a near-linear increase in L under prolonged irradiation duration. Both observed trends are consistent with the previously published results for p-type Ga_2O_3.[1–3] The activation energy $\Delta E_{A,I} = 68$ meV, obtained in this work, is comparable to that for p-Ga_2O_3 homoepitaxially grown on (010) Fe-doped substrates (72 meV).[3] Based on the determined $\Delta E_{A,I}$, the gallium vacancy-related acceptor concentration, N_A, was calculated as 1.15×10^{18} cm^{-3}.

To further elucidate the material's optoelectronic properties, temperature-dependent cathodoluminescence measurements were performed on the same undoped p-type Ga_2O_3 epitaxial layers. An activation energy (ΔE_A) of 344 meV, associated with electron irradiation-induced of CL intensity decay, was determined. This ΔE_A aligns well with gallium vacancy-related defect levels within the 300–500 meV range reported in Ref. 37, as well as agreeing with the previous study on homoepitaxial p-type Ga_2O_3 grown on an insulating (010) substrate.[5] The presence and characteristics of these defects, as evidenced by their distinct impacts on both carrier diffusion length and radiative efficiency, are critical considerations for the future development and optimization of Ga_2O_3-based electronic and optoelectronic devices.

In summary, p-type Ga_2O_3 homoepitaxial layers grown on (010)[3,5] and (001) (this work) gallium oxide substrates exhibit the same types of defects as evidenced from the temperature-dependent EBIC and CL measurements. The energetic locations for these defects differ from that for highly resistive (p) Ga_2O_3 layers.[2] This is possibly related to the difference in native defect concentrations for p[2] vs p-type[3,5] (this work) gallium oxide epitaxial layers.

SUPPLEMENTARY MATERIAL

Supplementary material describes electrical characterization of p–n junction structures grown in this work. Figure S1 shows a schematic of the structure used for capacitance–voltage (Fig. S2) and current–voltage (I–V) measurements (Fig. S3). The structure shows current rectification.

18 August 2025 00:33:35

AUTHOR DECLARATIONS

Conflict of Interest

The authors have no conflicts to disclose.

Author Contributions

Gabriel Marciaga: Data curation (equal); Formal analysis (equal); Writing – original draft (equal). **Jian-Sian Li:** Data curation (equal); Resources (equal). **Chao-Ching Chiang:** Data curation (equal); Resources (equal). **Fan Ren:** Conceptualization (equal); Methodology (equal); Resources (equal); Validation (equal). **Stephen J. Pearton:** Conceptualization (lead); Formal analysis (lead); Resources (lead); Validation (lead); Writing – review & editing (lead). **Corinne Sartel:** Data curation (equal); Resources (equal); Validation (equal). **Zeyu Chi:** Conceptualization (equal); Formal analysis (equal); Methodology (equal); Validation (equal). **Yves Dumont:** Conceptualization (equal); Methodology (equal); Validation (equal). **Ekaterine Chikoidze:** Conceptualization (lead); Methodology (lead); Resources (lead); Supervision (lead). **Alfons Schulte:** Conceptualization (equal); Methodology (equal); Validation (equal). **Arie Ruzin:** Conceptualization (equal); Validation (equal). **Leonid Chernyak:** Conceptualization (lead); Data curation (lead); Formal analysis (lead); Funding acquisition (lead); Investigation (lead); Methodology (lead); Project administration (lead); Resources (lead); Supervision (lead); Writing – original draft (lead); Writing – review & editing (lead).

DATA AVAILABILITY

The data that support the findings of this study are available within the article.

REFERENCES

[1] S. Modak, A. Ruzin, A. Schulte, and L. Chernyak, "Influence of energetic particles and electron injection on minority carrier transport properties in gallium oxide," Condens. Matter **9**, 2 (2024).

[2] S. Modak, A. Schulte, C. Sartel, V. Sallet, Y. Dumont, E. Chikoidze, X. Xia, F. Ren, S. J. Pearton, A. Ruzin, and L. Chernyak, "Impact of radiation and electron trapping on minority carrier transport in p-Ga$_2$O$_3$," Appl. Phys. Lett. **120**, 233503 (2022).

[3] L. Chernyak, S. Lovo, J.-S. Li, C.-C. Chiang, F. Ren, S. J. Pearton, C. Sartel, Z. Chi, Y. Dumont, E. Chikoidze, A. Schulte, A. Ruzin, and U. Shimanovich, "EBIC studies of minority electron diffusion length in undoped p-type gallium oxide," AIP Adv. **14**, 115301 (2024).

[4] S. M. Sze, *Physics of Semiconductor Devices* (John Wiley & Sons, New York, 1969).

[5] L. Chernyak, A. Schulte, J.-S. Li, C.-C. Chiang, F. Ren, S. J. Pearton, C. Sartel, V. Sallet, Z. Chi, Y. Dumont, E. Chikoidze, and A. Ruzin, "Cathodoluminescence studies of electron injection effects in p-type gallium oxide," AIP Adv. **14**, 085103 (2024).

[6] L. Chernyak, W. Burdett, M. Klimov, and A. Osinsky, "Cathodoluminescence studies of the electron injection-induced effects in GaN," Appl. Phys. Lett. **82**, 3680 (2003).

[7] L. Chernyak, A. Osinsky, H. Temkin, J. W. Yang, Q. Chen, and M. Asif Khan, "Electron beam induced current measurements of minority carrier diffusion length in gallium nitride," Appl. Phys. Lett. **69**, 2531 (1996).

[8] L. Chernyak, A. Osinsky, V. Fuflyigin, and E. F. Schubert, "Electron beam-induced increase of electron diffusion length in p-type GaN and AlGaN/GaN superlattices," Appl. Phys. Lett. **77**, 875 (2000).

[9] S. Modak, J. Lee, L. Chernyak, J. Yang, F. Ren, S. J. Pearton, S. Khodorov, and I. Lubomirsky, "Electron injection-induced effects in Si-doped β-Ga$_2$O$_3$," AIP Adv. **9**, 015127 (2019).

[10] E. B. Yakimov, A. Y. Polyakov, I. V. Shchemerov, N. B. Smirnov, A. A. Vasilev, P. S. Vergeles, E. E. Yakimov, A. V. Chernykh, F. Ren, and S. J. Pearton, "Experimental estimation of electron–hole pair creation energy in β-Ga$_2$O$_3$," Appl. Phys. Lett. **118**, 202106 (2021).

[11] E. B. Yakimov, A. Y. Polyakov, I. V. Shchemerov, N. B. Smirnov, A. A. Vasilev, A. I. Kochkova, P. S. Vergeles, E. E. Yakimov, A. V. Chernykh, M. Xian, F. Ren, and S. J. Pearton, "On the nature of photosensitivity gain in Ga$_2$O$_3$ Schottky diode detectors: Effects of hole trapping by deep acceptors," J. Alloys Compd. **879**, 160394 (2021).

[12] S. Modak, L. Chernyak, A. Schulte, C. Sartel, V. Sallet, Y. Dumont, E. Chikoidze, X. Xia, F. Ren, S. Pearton, A. Ruzin, D. Zhigunov, S. Kosolobov, and V. Drachev, "Variable temperature probing of minority carrier transport and optical properties in p-Ga$_2$O$_3$," APL Mater. **10**, 031106 (2022).

[13] J. Lee, E. Flitsiyan, L. Chernyak, J. Yang, F. Ren, S. J. Pearton, B. Meyler, and Y. J. Salzman, "Effect of 1.5 MeV electron irradiation on β-Ga$_2$O$_3$ carrier lifetime and diffusion length," Appl. Phys. Lett. **112**, 082104 (2018).

[14] S. Modak, L. Chernyak, A. Schulte, M. Xian, F. Ren, S. J. Pearton, A. Ruzin, S. S. Kosolobov, and V. P. Drachev, "Temperature dependence of cathodoluminescence emission in irradiated Si-doped β-Ga$_2$O$_3$," AIP Adv. **11**, 125014 (2021).

[15] J. I. Pankove, *Optical Processes in Semiconductors* (Prentice-Hall, Englewood Cliffs, NJ, 1971).

[16] O. Lopatiuk-Tirpak, L. Chernyak, F. X. Xiu, J. L. Liu, S. Jang, F. Ren, S. J. Pearton, K. Gartsman, Y. Feldman, A. Osinsky, and P. Chow, "Studies of minority carrier diffusion length increase in p-type ZnO:Sb," J. Appl. Phys. **100**, 086101 (2006).

[17] S. Modak, L. Chernyak, M. Xian, F. Ren, S. J. Pearton, S. Khodorov, I. Lubomirsky, A. Ruzin, and Z. Dashevsky, "Effect of electron injection on minority carrier transport properties in unintentionally doped GaN," J. Appl. Phys. **128**, 085702 (2020).

[18] S. Nakagomi, T. Momo, S. Takahashi, and Y. Kokubun, "Deep ultraviolet photodiodes based on β-Ga$_2$O$_3$/SiC heterojunction," Appl. Phys. Lett. **103**, 072105 (2013).

[19] S. Nakagomi, T.-a. Sato, Y. Takahashi, and Y. Kokubun, "Deep ultraviolet photodiodes based on the β-Ga$_2$O$_3$/GaN heterojunction," Sens. Actuators A **232**, 208 (2015).

[20] Y. Kokubun, S. Kubo, and S. Nakagomi, "All-oxide p–n heterojunction diodes comprising p-type NiO and n-type β-Ga$_2$O$_3$," Appl. Phys. Express **9**, 091101 (2016).

[21] J. Montes, C. Yang, H. Fu, T.-H. Yang, K. Fu, H. Chen, J. Zhou, X. Huang, and Y. Zhao, "Demonstration of mechanically exfoliated β-Ga$_2$O$_3$/GaN p–n heterojunction," Appl. Phys. Lett. **114**, 162103 (2019).

[22] H. H. Gong, X. H. Chen, Y. Xu, F.-F. Ren, S. L. Gu, and J. D. Ye, "A 1.86-kV double-layered NiO/β-Ga$_2$O$_3$ vertical p–n heterojunction diode," Appl. Phys. Lett. **117**, 022104 (2020).

[23] A. Y. Polyakov, V. I. Nikolaev, S. A. Tarelkin, A. I. Pechnikov, S. I. Stepanov, A. E. Nikolaev, I. V. Shchemerov, E. B. Yakimov, N. V. Luparev, M. S. Kuznetsov, A. A. Vasilev, A. I. Kochkova, M. I. Voronova, M. P. Scheglov,

18 August 2025 00:33:35

J. Kim, and S. J. Pearton, "Electrical properties and deep trap spectra in Ga$_2$O$_3$ films grown by halide vapor phase epitaxy on p-type diamond substrates," J. Appl. Phys. **129**, 185701 (2021).

[24] V. G. T. Vangipuram, K. Zhang, D. S. Yu, L. Meng, C. Chae, Y. Xu, J. Hwang, W. Lu, and H. Zhao, "Ultrawide bandgap LiGa$_5$O$_8$/β-Ga$_2$O$_3$ heterojunction p–n diodes," APL Electron. Devices **1**, 016115 (2025).

[25] W. Hao, Q. He, K. Zhou, G. Xu, W. Xiong, X. Zhou, G. Jian, C. Chen, X. Zhao, and S. Long, "Low defect density and small curve hysteresis in NiO/ β-Ga$_2$O$_3$ pn diode with a high PFOM of 0.65 GW/cm^2," Appl. Phys. Lett. **118**, 043501 (2021).

[26] J.-S. Li, C.-C. Chiang, X. Xia, T. J. Yoo, F. Ren, H. Kim, and S. J. Pearton, "Demonstration of 4.7 kV breakdown voltage in NiO/β-Ga$_2$O$_3$ vertical rectifiers," Appl. Phys. Lett. **121**, 042105 (2022).

[27] Y. Gao, X. Tian, Q. Feng, X. Lu, C. Zhang, J. Zhang, and Y. Hao, "Tuning electronic properties in tin-assisted n-type ϵ-Ga$_2$O$_3$:Zr thin films via PLD for p–n heterojunction," Appl. Surf. Sci. **616**, 156457 (2023).

[28] M. Xiao, B. Wang, J. Spencer, Y. Qin, M. Porter, Y. Ma, Y. Wang, K. Sasaki, M. Tadjer, and Y. Zhang, "NiO junction termination extension for high-voltage (>3 kV) Ga$_2$O$_3$ devices," Appl. Phys. Lett. **122**, 183501 (2023).

[29] J.-S. Li, H.-H. Wan, C.-C. Chiang, T. J. Yoo, M.-H. Yu, F. Ren, H. Kim, Y.-T. Liao, and S. J. Pearton, "Breakdown up to 13.5 kV in NiO/β-Ga$_2$O$_3$ vertical heterojunction rectifiers," ECS J. Solid State Sci. Technol. **13**, 035003 (2024).

[30] K. Yamamura, L. Zhu, C. P. Irvine, J. A. Scott, M. Singh, A. Jallandhra, V. Bansal, M. R. Phillips, and C. Ton-That, "Defect compensation in nitrogen-doped β-Ga$_2$O$_3$ nanowires: Implications for bipolar nanoscale devices," ACS Appl. Nano Mater. **5**, 12087 (2022).

[31] C.-Y. Huang, X.-Y. Tsai, F.-G. Tarntair, C. Langpoklakpam, T. S. Ngo, P.-J. Wang, Y.-C. Kao, Y.-K. Hsiao, N. Tumilty, H.-C. Kuo, T.-L. Wu, C.-L. Hsiao, and R.-H. Horng, "Heteroepitaxially grown homojunction gallium oxide PN diodes using ion implantation technologies," Mater. Today Adv. **22**, 100499 (2024).

[32] C. Liu, Z. Wu, H. Zhai, J. Hoo, S. Guo, J. Wan, J. Kang, J. Chu, and Z. Fang, "N-doped β-Ga$_2$O$_3$/Si-doped β-Ga$_2$O$_3$ linearly-graded p–n junction by a one-step integrated approach," J. Mater. Sci. Technol. **209**, 196 (2025).

[33] I. Zhelezova, I. Makkonen, and F. Tuomisto, "On the nature of as-grown and irradiation-induced Ga vacancy defects in β-Ga$_2$O$_3$," J. Appl. Phys. **136**, 065702 (2024).

[34] A. Langørgen, L. Vines, and Y. Kalmann Frodason, "Perspective on electrically active defects in β-Ga$_2$O$_3$ from deep-level transient spectroscopy and first-principles calculations," J. Appl. Phys. **135**, 195702 (2024).

[35] S. J. Pearton, J. Yang, P. H. Cary, F. Ren, J. Kim, M. J. Tadjer, and M. A. Mastro, "A review of Ga$_2$O$_3$ materials, processing, and devices," Appl. Phys. Rev. **5**, 011301 (2018).

[36] J. Y. Tsao, S. Chowdhury, M. A. Hollis, D. Jena, N. M. Johnson, K. A. Jones, R. J. Kaplar, S. Rajan, C. G. Van de Walle, E. Bellotti, C. L. Chua, R. Collazo, M. E. Coltrin, J. A. Cooper, K. R. Evans, S. Graham, T. A. Grotjohn, E. R. Heller, M. Higashiwaki, M. S. Islam, P. W. Juodawlkis, M. A. Khan, A. D. Koehler, J. H. Leach, U. K. Mishra, R. J. Nemanich, R. C. N. Pilawa-Podgurski, J. B. Shealy, Z. Sitar, M. J. Tadjer, A. F. Witulski, M. Wraback, and J. A. Simmons, "Ultrawide-bandgap semiconductors research opportunities and challenges," Adv. Electron. Mater. **4**, 1600501 (2018).

[37] M. Labed, N. Sengouga, C. Venkata Prasad, M. Henini, and Y. S. Rim, "On the nature of majority and minority traps in β-Ga$_2$O$_3$: A review," Mater. Today Phys. **36**, 101155 (2023).

[38] M. Higashiwaki, K. Sasaki, H. Murakami, Y. Kumagai, A. Koukitu, A. Kuramata, T. Masui, and S. Yamakoshi, "Recent progress in Ga$_2$O$_3$ power devices," Semicond. Sci. Technol. **31**, 034001 (2016).

[39] A. Kuramata, K. Koshi, S. Watanabe, Y. Yamaoka, T. Masui, and S. Yamakoshi, "High-quality β-Ga$_2$O$_3$ single crystals grown by edge-defined film-fed growth," Jpn. J. Appl. Phys. **55**, 1202A2 (2016).

[40] A. Y. Polyakov, I. H. Lee, N. B. Smirnov, E. B. Yakimov, I. V. Shchemerov, A. V. Chernykh, A. I. Kochkova, A. A. Vasilev, F. Ren, P. H. Carey, and S. J. Pearton, "Hydrogen plasma treatment of β-Ga$_2$O$_3$: Changes in electrical properties and deep trap spectra," Appl. Phys. Lett. **115**, 032101 (2019).

[41] A. Y. Polyakov, N. B. Smirnov, I. V. Shchemerov, S. J. Pearton, F. Ren, A. V. Chernykh, P. B. Lagov, and T. V. Kulevoy, "Hole traps and persistent photocapacitance in proton irradiated β-Ga$_2$O$_3$ films doped with Si," APL Mater. **6**, 096102 (2018).

[42] E. Chikoidze, C. Sartel, H. Mohamed, I. Madaci, T. Tchelidze, M. Modreanu, P. Vales-Castro, C. Rubio, C. Arnold, V. Sallet, Y. Dumont, and A. Perez-Tomas, "Enhancing the intrinsic p-type conductivity of the ultra-wide bandgap Ga$_2$O$_3$ semiconductor," J. Mater. Chem. C **7**, 10231–10239 (2019).

[43] K. Irmscher, Z. Galazka, M. Pietsch, R. Uecker, and R. Fornari, "Electrical properties of β-Ga$_2$O$_3$ single crystals grown by the Czochralski method," J. Appl. Phys. **110**, 063720 (2011).